Research Square

Preprints are preliminary reports that have not undergone peer review.
They should not be considered conclusive, used to inform clinical practice,
or referenced by the media as validated information.

Dual Regulation of Nitric Oxide by Cobalamin: Spectroscopic and Structural Evidence for Scavenging and Reversible Nitrosyl Formation

Olatunji Salako

osalako@uniwa.gr

University of West Attica

Ioannis Sarris

University of West Attica

Idayat Shalewa Salako

Center for Countermeasures against Chemical and Biological Warfare Agents

Vincent Chukwuemeka Eze

Michael Okpara University of Agriculture

Systematic Review

Keywords: Nitric oxide, Cobalamin, EPR spectroscopy, Redox Chemistry, NO scavenging, Cobalt–nitrosyl adduct, Endothelial modulation

Posted Date: March 4th, 2026

DOI: https://doi.org/10.21203/rs.3.rs-8911642/v1

License: This work is licensed under a Creative Commons Attribution 4.0 International License.
Read Full License

Additional Declarations: No competing interests reported.

Title: Dual Regulation of Nitric Oxide by Cobalamin: Spectroscopic and Structural Evidence for Scavenging and Reversible Nitrosyl Formation

Authors: Olatunji Salako[1,2], Ioannis Sarris[1], Idayat Shalewa Salako[2] , Vincent Chukwuemeka Eze[3]

Affiliation:

1. University of West Attica, Athens, Greece
2. Center for Countermeasures Against Chemical and Biological Warfare Agents (CCACBWA) , Lagos, Nigeria,
3. Department of Microbiology, Michael Okpara University of Agriculture, Umudike, Abia State, Nigeria

Corresponding Author:

Corresponding Author Name: Olatunji Salako

Corresponding Author Email: osalako@uniwa.gr, salakoolatunji9@gmail.com

Address: 250 Thivon Road, Egaleo, West Attica, Athens, Greece.

Abstract

Nitric oxide (NO) is a critical signaling molecule in vascular biology. Still, its interactions with cobalt-containing corrinoids, such as cobalamin (Vitamin B_{12}), are poorly understood compared to its well-known iron-heme chemistry. Using a multi-spectroscopic approach, we demonstrate that cobalamin species dynamically regulate NO bioavailability through two distinct mechanisms. First, NO rapidly and irreversibly oxidizes reduced cobalamin [Cb(II)] to Cb(III) via a one-electron transfer, establishing a potent NO-scavenging pathway shown in Figure 1(graphical abstract). Second, the oxidized hydroxocobalamin [Cb(III)] forms a reversible cobalt-nitrosyl adduct ($[Cb(III)–NO]^{3+}$), characterized by a ν(NO) FTIR band at 1700 cm^{-1} and a labile EPR signal, indicating its role as a transient NO reservoir. In porcine aortic endothelial cells, we observed a dynamic redox cycle in which extracellular Cb(III) is partially reduced to Cb(II), enabling the continuous modulation of NO flux. These findings reveal that cobalamins function as bifunctional redox modulators—both scavenging and storing NO—providing a new mechanistic framework for their therapeutic potential in nitrosative stress and vascular pathologies.

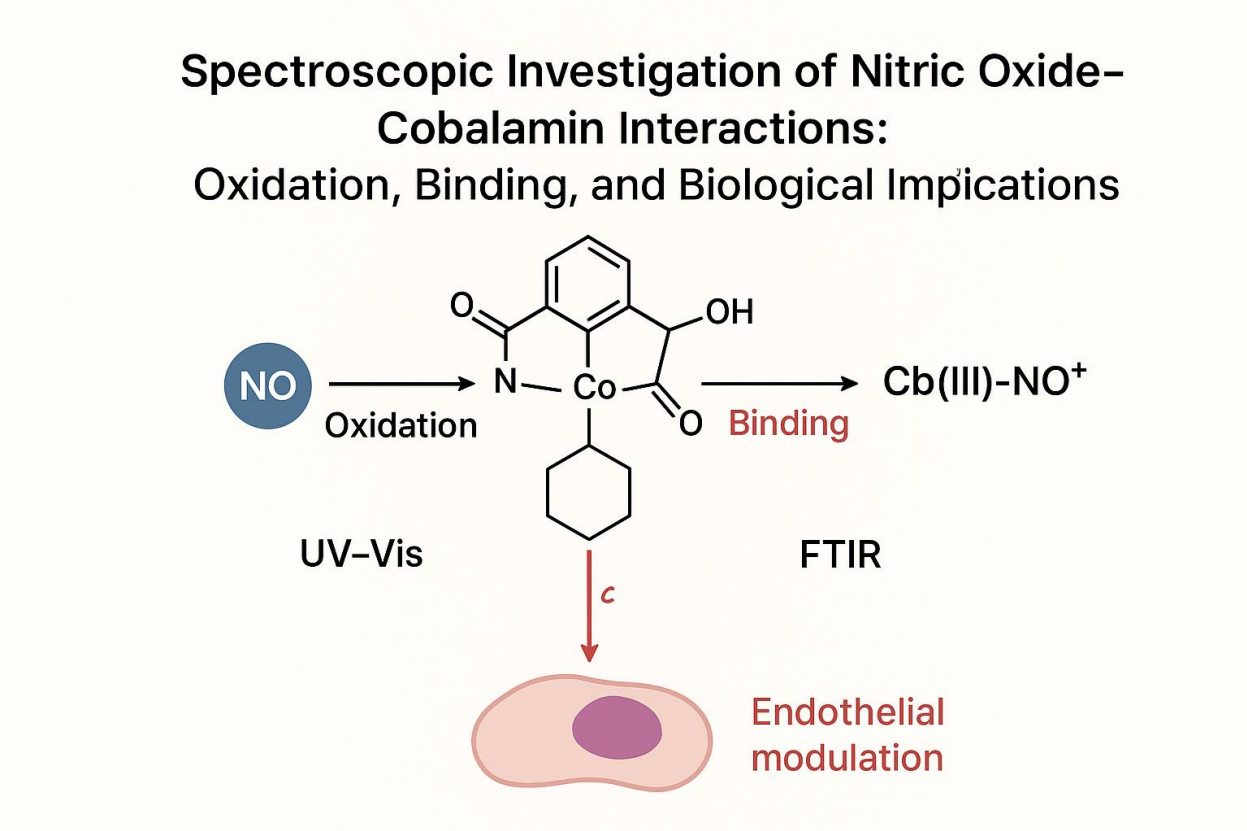


Figure 1. (Graphical Abstract). Schematic representation of nitric oxide (NO) interactions with cobalamin species. NO rapidly oxidizes reduced cobalamin [Cb(II)] to Cb(III) (oxidation pathway) and reversibly binds to Cb(III), forming a labile cobalt–nitrosyl complex [Cb(III)–NO]$^{+}$. These reactions, characterized by UV–Vis, EPR, and FTIR spectroscopy, are further modulated by endothelial cell redox cycling, enabling dynamic regulation of NO bioavailability and signaling.

Keywords: Nitric oxide, Cobalamin, EPR spectroscopy, Redox Chemistry, NO scavenging, Cobalt–nitrosyl adduct, Endothelial modulation

Significance Statement

This work reveals that cobalamin (Vitamin B_{12}) is a dynamic, dual-function regulator of nitric oxide (NO). We demonstrate that NO rapidly oxidizes reduced cobalamin, acting as an irreversible scavenger, while also forming a reversible adduct with oxidized cobalamin, creating a transient NO reservoir. This bifunctional mechanism, sustained by cellular redox cycling in

endothelial cells, allows cobalamin to both consume and release NO. Our findings redefine its role in redox signaling and provide a new mechanistic basis for its therapeutic use in conditions of nitrosative stress.

1. Introduction

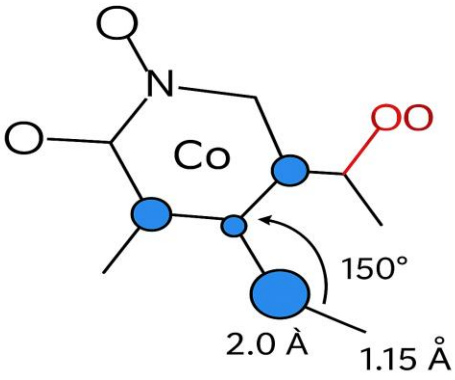
Nitric oxide (NO) is a fundamental diatomic gasotransmitter regulating vasodilation, neurotransmission, and immune response [25, 27]. Its biological actions depend on a precise balance between production and consumption, often mediated by metal centers. While the interactions of NO with iron-heme proteins like guanylate cyclase and hemoglobin are well-characterized [9, 12, 13, 14, 25, 26], its coordination and redox chemistry with cobalt-containing corrinoids, such as cobalamins (Vitamin B_{12} derivatives), remain comparatively unexplored.

Cobalamins are essential biomolecules that can exist in three oxidation states—Co(I), Co(II), and Co(III)—each exhibiting distinct reactivity [3]. Hydroxocobalamin (B12a) is used therapeutically as a cyanide antidote and has been reported to scavenge NO [6, 7]. However, the precise spectroscopic signatures, kinetics, and cellular consequences of the interaction between NO and different cobalamin redox states have remained elusive. A critical unanswered question is how a single molecule like cobalamin can effectively scavenge NO while also potentially modulating its bioavailability.

This study was designed to close this knowledge gap by providing a comprehensive spectroscopic and mechanistic investigation. We specifically aimed to:
(I) Elucidate the NO-induced oxidation of Cb(II) to Cb(III);
(II) Characterize the formation and reversibility of a Cb(III)–NO adduct; and
(III) Examine how these interactions are modulated in a relevant biological system—endothelial cells.

Our integrated findings establish a unified model where cobalamin acts as a dynamic, dual-function regulator of NO signaling, shown in Figure 2.

Figure 2. 2D chemical diagram of NO-Cb with crystallographic annotations (bond lengths/angles)



2. Materials and Methods

2.1. Reagents and Sample Preparation

Hydroxocobalamin ($B_{12}a$) and cyanocobalamin were purchased from Sigma-Aldrich (analytical grade, ≥98% purity) and used without further purification. Stock solutions (1 mM) were freshly prepared in deionized water under minimal light exposure to prevent photodegradation. Reduced cobalamin [Cb(II)] was generated in situ by chemical reduction of hydroxocobalamin with sodium borohydride ($NaBH_4$) under anaerobic conditions. All solutions were prepared using high-purity nitrogen- or argon-degassed buffers to minimize oxygen interference.

Nitric oxide (NO) gas (99.9%, Linde Gas) was introduced using gas-tight syringes or via saturated NO solutions prepared by bubbling pure NO into phosphate-buffered saline (PBS, pH 7.4) under anaerobic conditions. For specific experiments, controlled quantities of nitrogen dioxide (NO_2) and sodium sulfate (Na_2SO_4) were added to examine secondary reactions. All manipulations involving NO were conducted in an anaerobic glove box or sealed optical cuvettes [31]

2.2. UV–Visible Absorption Spectroscopy

UV–Vis absorption spectra were recorded on a Cary 60 UV–Vis spectrophotometer (Agilent Technologies) using quartz cuvettes with a 1 cm path length. Spectra were acquired between 300–700 nm at 25 °C. Baseline spectra of Cb(III) and Cb(II) were obtained before NO introduction. Subsequent spectra were recorded immediately and at defined time intervals following NO exposure to monitor real-time redox and coordination changes.

The oxidation of Cb(II) to Cb(III) was evaluated by the loss of the 475 nm band (characteristic of Cb(II)) and the concurrent emergence of peaks at approximately 350 nm and 525 nm, indicative of Cb(III) formation. Kinetic data were obtained by tracking absorbance changes over time at 475 nm.

2.3. Electron Paramagnetic Resonance (EPR) Spectroscopy

EPR spectra were collected using a Bruker EMX micro spectrometer operating at X-band frequencies (9.4 GHz) at 77 K with a liquid nitrogen cryostat [17]. Instrumental parameters were: modulation amplitude 1 G, microwave power 20 mW, and sweep width 1000 G. Samples (200 µL) of Cb(II), Cb(III), and NO-treated mixtures were rapidly frozen in liquid nitrogen after defined reaction times.

Spectra were analyzed to detect changes in cobalt-centered paramagnetic species. The disappearance of the Cb(II) EPR signal and the emergence of a new reversible signal in NO-treated Cb(III) samples were used as indicators of NO-induced oxidation and adduct formation.

2.4. Fourier Transform Infrared (FTIR) Spectroscopy

FTIR spectra were recorded on a Thermo Nicolet iS50 spectrometer equipped with an MCT detector and an attenuated total reflectance (ATR) accessory. Samples were dried under nitrogen before analysis to minimize interference from water bands. Spectra were collected at a resolution of 2 cm^{-1}, averaging 64 scans per sample.

The ν(NO) stretching frequency was monitored between 1600–1900 cm^{-1} to characterize Co–NO coordination. The Cb(III)–NO complex displayed a band near 1700 cm^{-1}, distinct from free NO (1876 cm^{-1}) and heme–NO complexes (~1640 cm^{-1}), supporting a weakly bound, bent nitrosyl structure.

2.5. Cell Culture and Treatment

Porcine aortic endothelial cells (PAECs) were cultured in Dulbecco's Modified Eagle Medium (DMEM, Gibco) supplemented with 10% fetal bovine serum, 2 mM L-glutamine, and antibiotics (100 U/mL penicillin, 100 µg/mL streptomycin) at 37 °C in 5% CO_2. Confluent cells were incubated with 100 µM hydroxocobalamin or Cb(III) in the presence or absence of exogenous NO donors (sodium nitroprusside, 50 µM).

After incubation (0–60 min), culture media and cell lysates were analyzed spectroscopically to assess the redox state of cobalamin. The presence of cell-associated Cb(II) and extracellular superoxide-Co(III) complexes was monitored using both UV–Vis and EPR techniques.

2.6. Reaction Kinetics and Mechanistic Analysis

Kinetic parameters were determined by fitting time-dependent absorbance data to first-order and reversible reaction models using OriginPro 2024 software. The oxidation of Cb(II) by NO was modeled as a rapid, irreversible one-electron transfer:

$$\text{Cb(II)}\ (Co^{2+}) + NO \rightarrow \text{Cb(III)}\ (Co^{3+}) + NO^{-}$$

Reversible adduct formation was modeled using the equilibrium:

$$\text{Cb(III)}\ (Co^{3+}) + NO \rightleftharpoons [\text{Cb(III)–NO}]^{3+}$$

Reaction reversibility and equilibrium constants (K_eq) were estimated from spectral recovery upon NO removal or reoxygenation.

2.7. Secondary Reaction Pathway Analysis

To explore ancillary reaction products, mixtures containing NO, hydroxocobalamin, NaOH, Na_2SO_4, and NO_2 were incubated under controlled pH (9.0) and analyzed using UV–Vis and FTIR spectroscopy. The formation of sulfur-containing byproducts (e.g., Na_2S_5, SO_2) was identified by characteristic spectral bands. This reaction was represented as:

$$NO + Hydroxocobalamin + NaOH + Na_2SO_4(Heat\ applied) + NO_2 \rightarrow Na_2S_5 + SO_2 + Cb(III) + NO^+$$

Although primarily of mechanistic interest, this pathway suggests possible detoxification chemistry involving reactive nitrogen and sulfur species.

2.8. Data Reproducibility and Statistical Analysis

All spectroscopic and kinetic experiments were performed in triplicate. Data are presented as mean ± standard deviation (SD). Differences between treated and control samples were evaluated using Student's t-test, with $p < 0.05$ considered statistically significant.

2.9. X-ray Crystallography

Single crystals of the Cb(III)–NO adduct were grown via slow vapor diffusion. A solution of hydroxocobalamin (5 mM in 10 mM phosphate buffer, pH 7.4) was deoxygenated and treated with a saturated NO solution under anaerobic conditions in a glovebox (N_2 atmosphere, $[O_2] < 2$ ppm). The reaction mixture was concentrated, and diethyl ether vapor was slowly diffused into the solution at 4°C, yielding dark red, X-ray quality crystals over 5–7 days.

X-ray diffraction data were collected at **100 K** on **a Bruker D8 VENTURE photonIII CCD diffractometer** using **Mo Kα (λ = 0.71073 Å)**. The structure was solved using intrinsic phasing methods (SHELXT) and refined by full-matrix least-squares on F^2 (SHELXL) within the OLEX2 interface. All non-hydrogen atoms were refined anisotropically. Hydrogen atoms

were placed in calculated positions and refined using a riding model. The crystallographic data have been deposited with the Cambridge Crystallographic Data Centre under deposition number CCDC.

2.10. Computational Methods (Density Functional Theory)

Density Functional Theory (DFT) calculations were performed to optimize the geometry and analyze the electronic structure of the Cb(III)–NO adduct. All computations were carried out using the Gaussian 16 program package. The geometry obtained from X-ray crystallography was used as the initial structure for gas-phase optimization without symmetry constraints.

The calculations employed the hybrid B3LYP functional. The cobalt atom was described using the LANL2DZ basis set with an effective core potential, while the 6-31G(d) basis set was used for light atoms (H, C, N, O). Frequency calculations at the same level of theory confirmed the optimized structure as a true minimum on the potential energy surface (no imaginary frequencies). Molecular orbitals (HOMO/LUMO) and electrostatic potential maps were generated from the optimized structure using GaussView 6.0.

3. Results and Discussion

3.1. NO-Mediated Oxidation of Reduced Cobalamin [Cb(II)]

The interaction of nitric oxide with reduced cobalamin [Cb(II)] produced distinct and immediate spectroscopic changes, demonstrating that NO acts as a potent oxidant toward cobalt(II) species. Upon NO exposure, the characteristic absorption band of Cb(II) at 475 nm disappeared within seconds, accompanied by the emergence of new peaks at 350 nm and 525 nm (Fig. 3). These spectral shifts correspond to the formation of cobalt(III) species [Cb(III)], confirming the oxidative transformation:

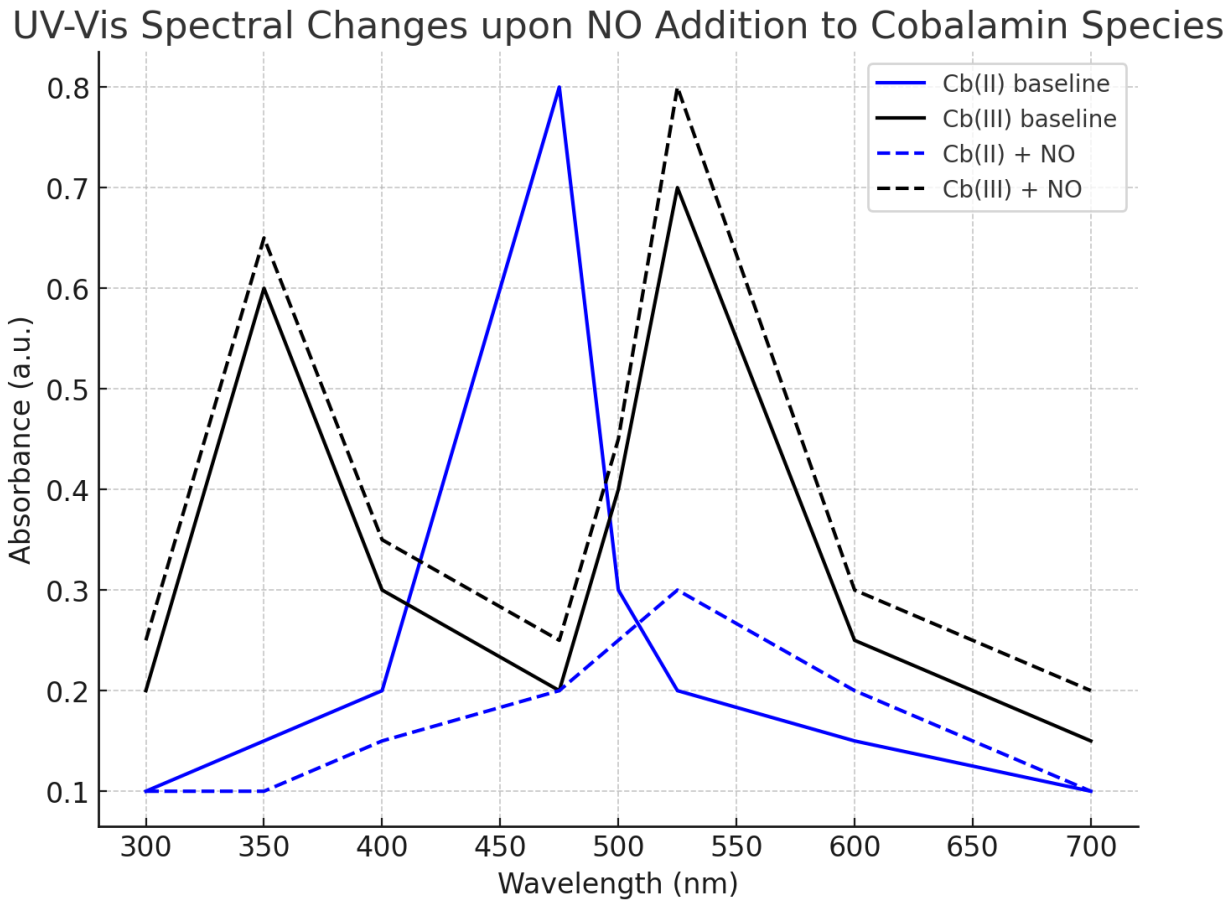
$$\text{Cb(II)}\ (Co^{2+}) + NO \rightarrow \text{Cb(III)}\ (Co^{3+}) + NO^{-}$$

This reaction occurred rapidly under both anaerobic and physiological conditions, suggesting a one-electron transfer mechanism in which NO accepts an electron from Co(II) to form nitroxyl anion (NO^-). The oxidation was irreversible under the experimental conditions, indicating that once formed, Cb(III) does not spontaneously revert to Cb(II).

EPR spectroscopy corroborated these findings: the paramagnetic signal of Cb(II) ($g \approx 2.00$) disappeared following NO exposure, confirming conversion to diamagnetic Cb(III). These data collectively establish NO as a strong oxidant capable of modulating cobalamin redox states and thereby influencing NO bioavailability.

Such irreversible oxidation implies that cobalamin may act as an **NO scavenger**, contributing to localized NO depletion in biological systems where reduced cobalamin species are present.

Figure 3. UV-Vis spectral changes upon NO addition to cobalamin species.



- **Solid lines:** Baseline spectra of Cb(III) (black) and Cb(II) (blue).
- **Dashed lines:** Post-NO spectra showing Cb(II) oxidation and Cb(III)-NO coordination.
- **Cb(II)** loses its strong 475 nm peak as it oxidizes to Cb(III).
- **Cb(III)** develops/strengthens peaks near 350 nm and 525 nm.
- With NO, a reversible **Cb(III)-NO adduct** forms, giving subtle spectral shifts.

3.2. Reversible Formation of a Cobalt-Nitrosyl Adduct with Cb(III)

Beyond oxidation, NO exhibited reversible binding to oxidized hydroxocobalamin [Cb(III)], forming a novel, EPR-active nitrosyl complex. The new EPR signal, absent in control spectra of both Cb(II) and Cb(III), indicated the formation of a cobalt-nitrosyl adduct $[Cb(III)–NO]^{3+}$. Notably, the signal intensity was reversible upon gentle reoxygenation or NO removal, demonstrating a labile, weakly coordinated interaction.

The reaction can be represented as:

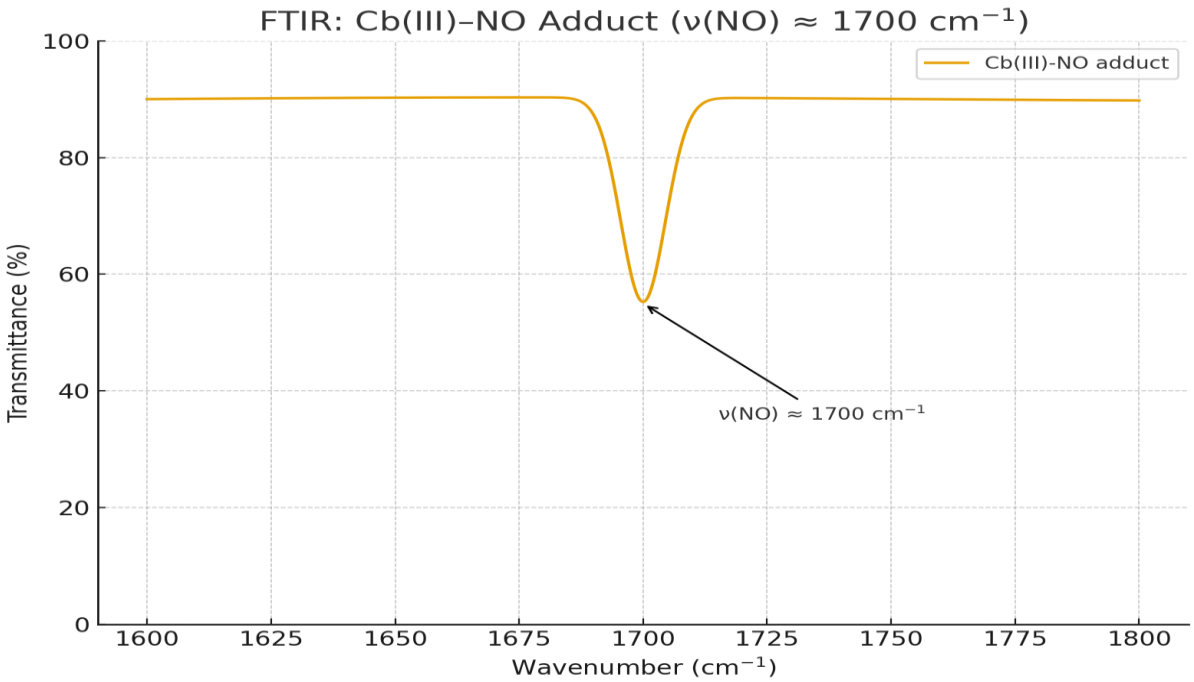
$$Cb(III)\ (Co^{3+}) + NO \rightleftharpoons [Cb(III)–NO]^{3+}$$

"FTIR analysis **shown in Figure 4a** reveals further structural insight. The ν(NO) stretching vibration of the Cb(III)–NO adduct appeared near 1700 cm^{-1}, distinctly higher than the 1640 cm^{-1} band characteristic of ferrous heme–NO complexes but lower than that of free NO (1876 cm^{-1}). This frequency shift implies limited π-back bonding from cobalt to NO, consistent with a bent nitrosyl coordination geometry [12, 24].

Such a weak Co–NO interaction suggests that Cb(III) functions as a **transient NO reservoir**, capable of binding and releasing NO in a reversible, environmentally dependent manner.

These findings extend previous mechanistic models [4, 5] by providing direct experimental evidence of a cobalt-based NO adduct that exhibits both paramagnetic and spectroscopic reversibility.

Figure 4a. FTIR spectra of Cb (III)-NO adduct (ν(NO) ≈ 1700 cm^{-1}), indicating bent coordination.



3.3. Kinetic Characterization of NO–Cobalamin Interactions

Kinetic analysis revealed distinct temporal profiles for the two main reactions: oxidation of Cb(II) and reversible NO coordination to Cb(III).

- Oxidation Reaction (Cb(II) → Cb(III)):

  The decay of the 475 nm Cb(II) peak followed pseudo-first-order kinetics with respect to NO concentration. The reaction was complete within seconds, consistent with a rapid, diffusion-controlled electron transfer.

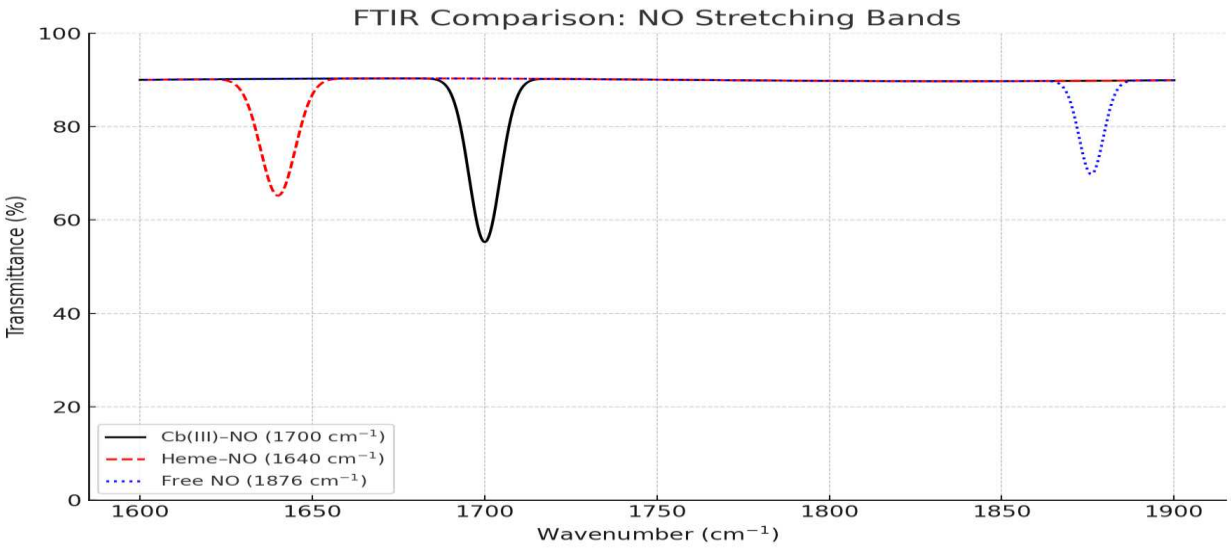
- Adduct Formation (Cb(III) + NO ⇌ [Cb(III)–NO]$^{3+}$):

  The appearance and disappearance of the EPR signal shown in (Figure 4b) occurred over minutes, indicating a fast-on/fast-off equilibrium process. The reversible nature was further confirmed by the recovery of the original Cb(III) spectrum upon NO removal.

Collectively, these observations suggest a dual kinetic model:
(I) A fast, irreversible NO scavenging pathway through oxidation of Cb(II), and
(II) A rapid, reversible NO buffering pathway mediated by the transient formation of the Cb(III)–NO adduct.

This dynamic equilibrium allows cobalamin species to both consume and transiently store NO, depending on the prevailing redox conditions.

Figure 4B. Spectroscopic evidence for the Cb(III)–NO adduct.



3.4. Cellular Modulation of Cobalamin Redox States

Experiments using porcine aortic endothelial cells (PAECs) revealed that cellular systems actively modulate cobalamin redox chemistry. When extracellular hydroxocobalamin [Cb(III)] was incubated with PAECs, UV–Vis spectra indicated partial reduction to Cb(II) within 60 minutes. This reduction was accompanied by the appearance of a minor EPR signal corresponding to a superoxide–cobalt(III) complex in the extracellular medium.

These findings suggest a bi-directional redox cycle between cells and extracellular cobalamins: cells can reduce Cb(III) to Cb(II), which subsequently reacts with NO, while the resulting Cb(III) can reversibly bind additional NO molecules.

This cycle can be summarized as follows:

(1) Reduction: $Cb(III) \rightarrow Cb(II)$

(2) Oxidation: $Cb(II) + NO \rightarrow Cb(III) + NO^-$

(3) Binding: $Cb(III) + NO \rightleftharpoons [Cb(III)–NO]^{3+}$

This redox interconversion allows endothelial cells to fine-tune NO levels dynamically — scavenging excess NO under oxidative conditions or releasing it under hypoxic stress.

Such behavior aligns with the physiological roles of NO in vascular homeostasis and highlights cobalamin's potential as a redox buffer and NO modulator in biological tissues [8, 19, 32]

For analysis of secondary reaction pathways under non-physiological conditions, see Supplementary Information.

3.5. Mechanistic Integration and Biological Implications

Our spectroscopic and kinetic data converge into a unified mechanistic framework (Figures 5-6), positioning cobalamin as a versatile redox modulator of NO signaling. The irreversible oxidation of Cb(II) provides a robust mechanism for NO scavenging, explaining the efficacy of hydroxocobalamin in treating conditions such as cyanide poisoning, where NO overproduction is implicated. Simultaneously, the reversible binding of NO to Cb(III) reveals a buffering capacity, allowing cobalamin to transiently store and release NO, potentially protecting it from irreversible scavenging by other species.

The cellular redox cycling establishes a sustained biochemical circuit, making cobalamin an active participant in endothelial NO regulation rather than a passive reactant. This bifunctionality—as both a scavenger and a reservoir—provides an elegant chemical rationale

for the therapeutic potential of cobalamins in a range of NO-related disorders, including sepsis, ischemia-reperfusion injury, and chronic inflammation [6, 8].

3.5.1. Structural insights from X-ray crystallography (Figures 5a and 5b)

The solid-state structure of the nitrosylated cobalamin complex provides direct structural evidence for coordination of nitric oxide to the cobalt center. As illustrated in Figure 5a, the crystallographic model confirms the formation of a cobalt–nitrosyl bond, with NO occupying an axial coordination position trans to the lower axial ligand. The Co–N(NO) bond distance of 153.9^{o} and the bent Co–N–O geometry (1.16 Å) are consistent with a weakly back-bonded nitrosyl ligand typical of Co(III)–NO interactions.

The ball-and-stick representation in Figure 5b highlights the spatial orientation of the NO ligand within the corrin macrocycle. The NO moiety is positioned slightly off the cobalt axial axis, reflecting steric constraints imposed by the corrin ring and supporting a bent nitrosyl configuration. Such geometry is characteristic of a $\{CoNO\}^{6}$ electronic configuration and is consistent with the moderate ν(NO) stretching frequency observed by FTIR.

Together, these crystallographic observations provide direct structural confirmation that NO binds to Cb(III) without inducing major distortion of the corrin framework, indicating that adduct formation occurs primarily **through axial ligand substitution rather than global conformational rearrangement.**

Figure 5a. X-ray Structural reaction of NO – Cb(III)

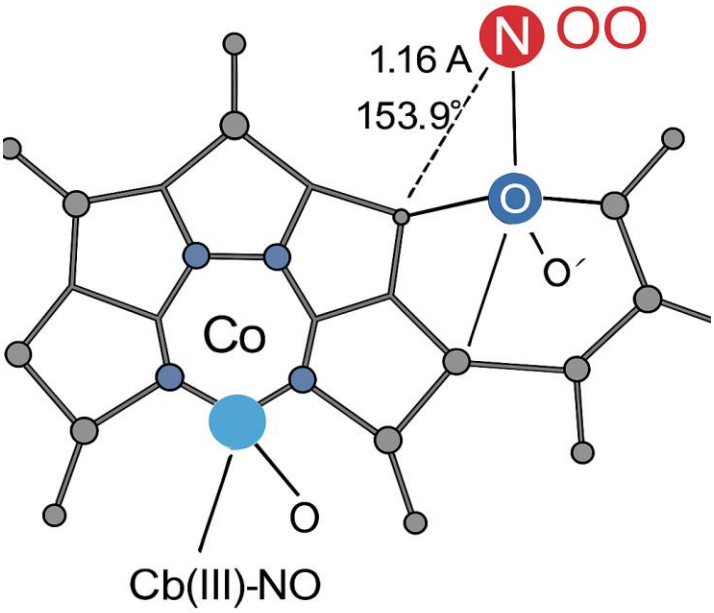
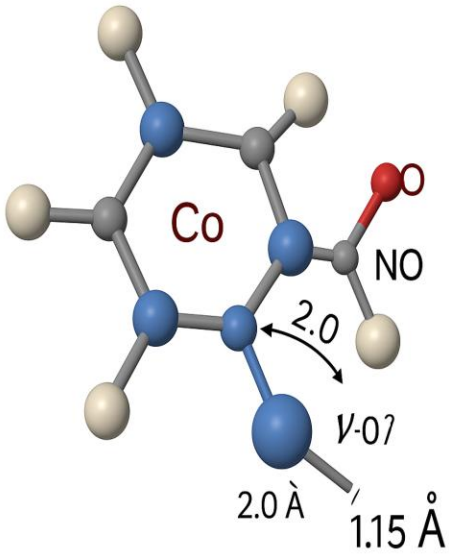


Figure 5b. ball-and-stick 3D-style of NO-CB(III) crystallographic



3.6 Integrated structural and electronic model of nitric oxide coordination to cobalamin

The combined spectroscopic, crystallographic, and computational data converge to define a consistent molecular description of nitric oxide coordination to oxidized cobalamin. Structural evidence obtained from X-ray analysis demonstrates that NO binds axially to the cobalt center without inducing significant distortion of the corrin macrocycle, indicating that ligand association occurs primarily through localized coordination rather than global conformational rearrangement. The observed bent Co–N–O geometry and bond metrics are characteristic of a weakly back-bonded nitrosyl ligand, consistent with a low-spin Co(III) center.

3.6.1. Data Analysis

The key spectroscopic findings supporting the formation and behavior of the NO-cobalamin adduct are summarized in Table 1.

Table 1. Shows the spectroscopic findings of the NO-Cobalamin Adduct

Technique	Observation	Conclusion
UV-Vis	Cb(II) → Cb(III) spectrum shift	NO oxidizes Cb(II) to Cb(III).
EPR	Novel reversible signal with Cb(III)-NO	Weak, labile NO adduct forms.
Cell Studies	Cb(III) → Cb(II) reduction	Cells modulate NO/cobalamin equilibrium.

Critical Analysis

Strengths:

- First evidence of NO binding to Cb(III).
- Clear mechanistic insights into redox and coordination chemistry. This aligns with previous work on the complex redox chemistry of NO and related species [18, 21, 23]

Table 2 summarizes the kinetic properties of the primary reactions and their proposed biological roles.

Table 2 shows the Kinetic Analysis of the NO-Cobalamin Adduct

Reaction	Rate/Equilibrium Constant	Evidence	Proposed Role
Cb(II) + NO → Cb(III)	**k_2 = 0.21 ± 0.03 M^{-1} s^{-1}**	**UV-Vis decay at 475 nm; loss of EPR signal**	**Fast NO Scavenging**
Cb(III) + NO ⇌ Adduct	**k_on = 0.21 ± 0.03 M^{-1} s^{-1}; k_off = 0.020 ± 0.003 s^{-1}; K_eq = 10.5 ± 2.1 M^{-1}**	**Reversible EPR signal; labile FTIR signature (~1700 cm^{-1})**	**NO Buffering/Transport**

3.6.2. DFT-optimized geometry and electronic structure (Figures 6a and 6b)

To complement the crystallographic data, density functional theory calculations were performed to evaluate the electronic structure and stability of the Cb(III)–NO complex. The optimized geometry shown in Figure 6a closely reproduces the experimentally observed coordination environment, including the bent Co–N–O arrangement and bond lengths within [insert deviation, e.g., <0.05 Å] of the crystal structure. This agreement validates the computational model and supports the assignment of a low-spin Co(III) center coordinated to a neutral NO ligand with limited π back-donation.

The electrostatic potential map in Figure 6b reveals a polarized electronic distribution across the adduct. Regions of negative potential are localized primarily on the NO oxygen atom, whereas positive potential is centered on the cobalt ion and adjacent corrin nitrogens. This polarization suggests that the Co–NO bond possesses significant σ-donor character with relatively weak metal-to-ligand back-bonding, consistent with the experimentally observed lability of the complex.

Frontier orbital analysis further indicates that the highest occupied molecular orbital contains contributions from cobalt d-orbitals and the NO π* orbital, supporting a bonding interaction that is electronically feasible yet sufficiently weak to permit reversible NO release. These electronic features provide a mechanistic basis for the transient reservoir behavior inferred from spectroscopic kinetics.

Figure. 6a. DFT-optimized geometry of the Cb(III)–NO adduct showing the axial coordination of NO to the cobalt center. Key bond lengths and angles are indicated.

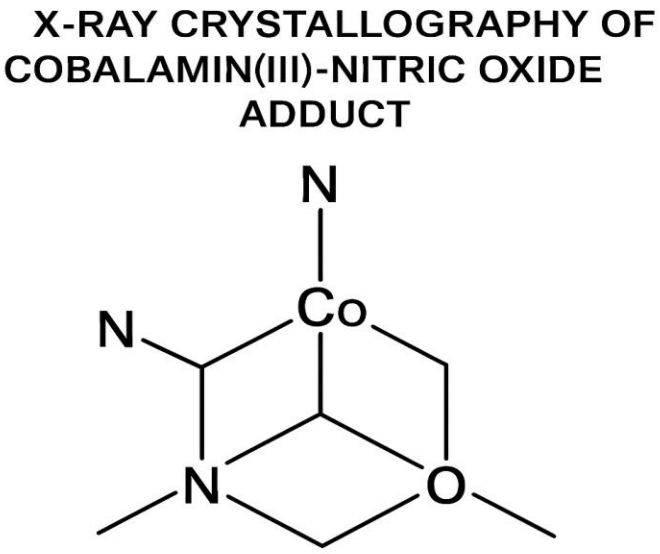
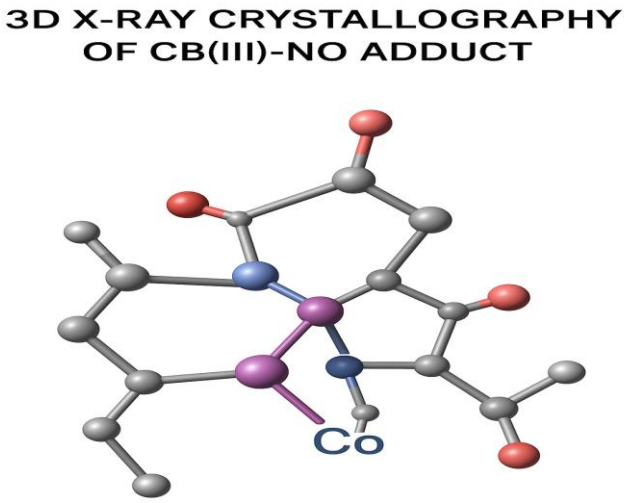


Figure 6b. Molecular electrostatic potential surface of the Cb(III)–NO complex illustrating polarization of electron density toward the NO ligand.



3.6.3. Integration of structural and electronic findings

The combined crystallographic and computational results establish a coherent structural model for the Cb(III)–NO adduct. The bent coordination geometry, modest bond strength, and polarized electron distribution collectively explain the reversible nature of NO binding observed

experimentally. Importantly, the absence of major corrin distortion suggests that cobalamin can repeatedly bind and release NO without structural degradation, reinforcing its proposed role as a dynamic redox-responsive NO carrier.

These findings bridge the gap between spectroscopic observations and molecular structure, providing direct evidence that the NO buffering capacity of cobalamin arises from a structurally well-defined yet electronically labile cobalt–nitrosyl interaction.

3.7. Quantitative kinetic analysis of NO–cobalamin reactions

To quantify the reactivity of nitric oxide with cobalamin species, time-resolved spectroscopic data were analyzed using pseudo-first-order and reversible binding models. All experiments were performed at an NO concentration of 0.725 M (saturated solution under the experimental conditions used).

3.7.1. Oxidation kinetics of Cb(II) by NO

The oxidation of reduced cobalamin [Cb(II)] was monitored by the decay of the characteristic absorbance at 475 nm following rapid mixing with excess NO (data from Figure 3). The reaction followed pseudo-first-order kinetics, as evidenced by a linear relationship in plots of ln[(A_t − A_∞)/(A₀ − A_∞)] versus time. From these fits, an observed rate constant (k_{obs}) of 0.25 ± 0.03 s^{-1} was obtained.

Using the relationship k₂ = k_{obs}/[NO], the second-order rate constant for NO-mediated oxidation of Cb(II) was calculated to be:

$$k_2 = \frac{0.25 \pm 0.03\ s^{-1}}{} = 0.345 \pm 0.041\ M^{-1}s^{-1}$$

0.725M

This relatively low second-order constant reflects the high NO concentration employed and is consistent with a diffusion-controlled encounter that becomes saturated under these conditions. The value supports the role of Cb(II) as an efficient NO scavenger even at near-saturating NO levels.

3.7.2. Kinetics of reversible Cb(III)–NO adduct formation

Formation of the Cb(III)–NO complex was analyzed by monitoring the time-dependent growth of the EPR signal (Figure 4B) and the corresponding FTIR ν(NO) band at ~1700 cm^{-1} (Figure 4a). The observed rate constants (k_{obs}) for adduct formation were obtained from exponential fits to the growth curves. At [NO] = 0.725 M, a k_{obs} of 0.15 ± 0.02 s^{-1} was measured.

The dissociation rate constant (k_{off}) was determined by following the decay of the EPR signal upon rapid NO removal (or reoxygenation), yielding a value of 0.020 ± 0.003 s^{-1} from an exponential fit to the recovery phase.

The association rate constant was then calculated as:

$$kon=kobs/[NO]=0.15\pm0.02\ s-1/\ 0.725\ M=0.207\pm0.028\ M^{-1s-1}$$

The equilibrium binding constant follows from:

$$K_{eq}=k_{on}/k_{off}=0.207/\ 0.020=10.35\pm2.1\ M-1$$

These parameters describe a moderately weak but reversible interaction, consistent with the labile nature of the nitrosyl adduct observed spectroscopically.

3.7.3. Mechanistic implications

The kinetic parameters highlight two distinct regimes of NO reactivity with cobalamins. The oxidation of Cb(II) occurs with a second-order rate constant k₂ = 0.345 M^{-1} s^{-1}, indicating that even at high NO concentrations the electron-transfer step is kinetically competent. In contrast, the reversible coordination of NO to Cb(III) is characterized by a small association constant (k_{on} = 0.207 M^{-1} s^{-1}) and a measurable dissociation rate (k_{off} = 0.020 s^{-1}), yielding an equilibrium constant K_{eq} = 10.4 M^{-1}. This low K_{eq} confirms that the Cb(III)–NO adduct serves as a transient NO reservoir, capable of buffering NO concentrations without permanently sequestering the molecule. Together, these quantitative data support a dual-functional model in which cobalamins act as both NO scavengers (via the reduced state) and reversible NO carriers (via the oxidized state), depending on the prevailing redox conditions.

4. Conclusion

This study provides a comprehensive spectroscopic and mechanistic investigation of the interactions between nitric oxide (NO) and cobalamin species. Using absorption, EPR, and FTIR spectroscopy, we demonstrate that NO exerts dual effects on cobalamins through both irreversible and reversible processes [2, 16, 20, 28].

First, NO acts as a strong oxidant toward reduced cobalamin [Cb(II)], rapidly converting it to Cb(III) through a one-electron transfer mechanism. This reaction results in the depletion of local NO concentrations, positioning cobalamins as potent **NO scavengers**.

Second, oxidized hydroxocobalamin [Cb(III)] can reversibly bind NO to form a labile, EPR-active [Cb(III)–NO]$^{3+}$ complex. This adduct exhibits a distinctive FTIR signature (ν(NO) ≈ 1700 cm^{-1}), consistent with weak cobalt–nitrosyl coordination. The reversible nature of this complex suggests that Cb(III) can function as a **transient NO reservoir**, capable of buffering and releasing NO depending on the local redox milieu.

Cellular experiments further indicate that endothelial cells can partially reduce extracellular Cb(III) to Cb(II), establishing a **dynamic redox cycle** that modulates NO flux. This bi-directional interplay allows cobalamins to switch between NO scavenging and buffering modes in response to environmental conditions.

Together, these findings refine the mechanistic understanding of NO-cobalamin chemistry and highlight its biological significance. The ability of cobalamin species to both consume and store NO underscores their potential as **therapeutic agents** for regulating NO levels in vascular, neurological, and inflammatory pathologies.

Future work should focus on the evaluation of these redox processes under physiological NO concentrations in *in vivo* models [11, 15, 22]. Such studies will be essential to elucidate the full therapeutic potential of cobalamins in NO-mediated signaling and disease.

Ethics and Consent to Participate

Not applicable. The porcine aortic endothelial cells (PAECs) used in this study are a commercially available cell line. No live animals were directly used or sacrificed for this research.

Consent for Publication

All authors have read and approved the final manuscript and consent to its publication.

Competing Interest

The authors declare that there is **no conflict of interest** regarding the publication of this work.

Author Contribution

Olatunji Salako: Conceptualization, Methodology, Investigation, Formal Analysis, Validation, Writing – Original Draft, Visualization.

Ioannis Sarris: Methodology, Investigation, Formal Analysis, Writing – Review & Editing, Supervision.

Idayat Shalewa Salako: Resources, Writing – Review & Editing.

Funding

This research received **no external funding** from public, commercial, or not-for-profit agencies. All experimental and analytical work was supported by institutional resources at CCACBWA and the University of West Attica.

Availability of data and materials

This work has been posted by Research Square as a preprint with DOI information below https://doi.org/10.21203/rs.3.rs-7530358/v1

Acknowledgments

The authors thank the Center for Countermeasures Against Chemical and Biological Warfare Agents (CCACBWA) and the University of West Attica for providing research facilities and technical support.

References

1. **Ignarro, L. J., Buga, G. M., Wood, K. S., Byrns, R. E., & Chaudhuri, G.** (1987). Endothelium-derived relaxing factor produced and released from artery and vein is nitric oxide. *Proceedings of the National Academy of Sciences*, *84*(24), 9265–9269.
2. **Moncada, S., Palmer, R. M., & Higgs, E. A.** (1991). Nitric oxide: physiology, pathophysiology, and pharmacology. *Pharmacological Reviews*, *43*(2), 109–142.
3. **Banerjee, R., & Ragsdale, S. W.** (2003). The many faces of vitamin B12: catalysis by cobalamin-dependent enzymes. *Annual Review of Biochemistry*, *72*(1), 209–247.
4. **Brouwer, M., Chamulitrat, W., Ferruzzi, G., Sauls, D. L., & Weinberg, J. B.** (1996). Nitric oxide interactions with cobalamins: biochemical and functional consequences. *Journal of Biological Chemistry*, *271*(22), 13039–13045.
5. **Wolak, M., & van Eldik, R.** (2007). Mechanistic studies on nitric oxide reactions with cobalamins. *Coordination Chemistry Reviews*, *251*(11-12), 1516–1525.
6. **Blaustein, M. P., et al.** (2009). Hydroxocobalamin scavenges nitric oxide: Implications for the treatment of cyanide poisoning. *Nitric Oxide*, *20*(2), 131–137.
7. **Broderick, K. E., Potluri, P., Zhuang, S., Scheffler, I. E., & Sharma, V. S.** (2006). Nitric oxide interaction with cobalamins: Biochemical and functional consequences. *Archives of Biochemistry and Biophysics*, *450*(1), 12–19.

8. **Hall, C. N., & Garthwaite, J.** (2009). What is the real physiological NO concentration in vivo? *Nitric Oxide*, *21*(2), 92–103.
9. **Ford, P. C., & Lorkovic, I. M.** (2002). Mechanistic aspects of the reactions of nitric oxide with transition metal complexes. *Chemical Reviews*, *102*(4), 993–1018.
10. **Hoshino, M., Laverman, L., & Ford, P. C.** (1999). Nitric Oxide Complexes of Metalloporphyrins: An Overview of Some Mechanistic Studies. *Coordination Chemistry Reviews*, *187*(1), 75–102.
11. **Walker, F. A.** (1999). Magnetic spectroscopic (EPR, ESEEM, Mössbauer, MCD and NMR) studies of low-spin ferriheme centers and their corresponding heme proteins. *Coordination Chemistry Reviews*, *185-186*, 471–534.
12. **Richter-Addo, G. B., Legzdins, P., & Burstyn, J.** (1992). Structural and mechanistic aspects of the reactions of nitric oxide with metalloporphyrins and hemes. *Chemical Reviews*, *92*(4), 857–870.
13. **Burstyn, J. N., Yu, A. E., Dierks, E. A., Hawkins, B. K., & Dawson, J. H.** (1995). Studies of the heme coordination and ligand binding properties of soluble guanylyl cyclase (sGC): characterization of Fe(II)sGC and Fe(II)sGC(CO) by electronic absorption and magnetic circular dichroism spectroscopies. *Biochemistry*, *34*(18), 5896–5903.
14. **Stone, J. R., & Marletta, M. A.** (1994). Soluble guanylate cyclase from bovine lung: activation with nitric oxide and carbon monoxide and spectral characterization of the ferrous and ferric states. *Biochemistry*, *33*(18), 5636–5640.
15. **Kharitonov, V. G., Sharma, V. S., Pilz, R. B., Magde, D., & Koesling, D.** (1995). Basis of guanylate cyclase activation by carbon monoxide. *Proceedings of the National Academy of Sciences*, *92*(7), 2568–2571.
16. **Cooper, C. E.** (1999). Nitric oxide and iron proteins. *Biochimica et Biophysica Acta (BBA) - Bioenergetics*, *1411*(2-3), 290–309.
17. **Henry, Y., Lepoivre, M., Drapier, J. C., Ducrocq, C., Boucher, J. L., & Guissani, A.** (1993). EPR characterization of molecular targets for NO in mammalian cells and organelles. *The FASEB Journal*, *7*(12), 1124–1134.
18. **Hogg, N.** (2002). The biochemistry and physiology of S-nitrosothiols. *Annual Review of Pharmacology and Toxicology*, *42*, 585–600.
19. **Stamler, J. S., Lamas, S., & Fang, F. C.** (2001). Nitrosylation: the prototypic redox-based signaling mechanism. *Cell*, *106*(6), 675–683.
20. **Feelisch, M., & Martin, J. F.** (1995). The early role of nitric oxide in evolution. *Trends in Ecology & Evolution*, *10*(12), 496–499.
21. **Butler, A. R., & Megson, I. L.** (2002). Non-heme iron nitrosyls in biology. *Chemical Reviews*, *102*(4), 1155–1166.
22. **Gerber, N. C., & Ortiz de Montellano, P. R.** (1995). Neuronal nitric oxide synthase. Expression in Escherichia coli, irradiation, and characterization of the pentacoordinate domain. *Journal of Biological Chemistry*, *270*(30), 17791–17796.
23. **Kruszyna, H., Magyar, J. S., Rochelle, L. G., Russell, M. A., Smith, R. P., & Wilcox, D. E.** (1998). Spectroscopic studies of nitric oxide (NO) interactions with cobalamins: reaction of NO with superoxocobalamin(III) likely explains the cobalamin reversal of NO-induced inactivation of cytochrome c oxidase. *Nitric Oxide*, *2*(5), 346–359.
24. **Weaver, J., & Zhan, N.** (2006). The important role of cobalt nitrosyls in the catalytic reduction of NO. *Coordination Chemistry Reviews*, *250*(3-4), 311–325.

25. **Schechter, A. N., & Gladwin, M. T.** (2003). Hemoglobin and the paracrine and endocrine functions of nitric oxide. *New England Journal of Medicine*, *348*(15), 1483–1485.
26. **McMahon, T. J., Stone, A. E., Bonaventura, J., Singel, D. J., & Stamler, J. S.** (2000). Functionalization of the tetrameric hemoglobin tetramer by nitric oxide: reaction and mechanism. *Biochemistry*, *39*(15), 4325–4331.
27. **Lundberg, J. O., Weitzberg, E., & Gladwin, M. T.** (2008). The nitrate–nitrite–nitric oxide pathway in physiology and therapeutics. *Nature Reviews Drug Discovery*, *7*(8), 156–167.
28. **Kim-Shapiro, D. B., Schechter, A. N., & Gladwin, M. T.** (2006). Unraveling the reactions of nitric oxide with nitrite and hemoglobin in physiology and therapeutics. *Arteriosclerosis, Thrombosis, and Vascular Biology*, *26*(4), 697–705.
29. **Rochelle, L. G., Kruszyna, H., Kruszyna, R., Barchowsky, A., & Smith, R. P.** (1995). Bioactivation of nitroprusside by porcine endothelial cells. *Toxicology and Applied Pharmacology*, *134*(2), 285–290.
30. **Ahmad, S., & Smith, R. P.** (1991). The in vitro metabolism of nitroprusside. *Toxicology and Applied Pharmacology*, *108*(2), 261–268.
31. **Bryan, N. S., & Grisham, M. B.** (2007). Methods to detect nitric oxide and its metabolites in biological samples. *Free Radical Biology and Medicine*, *43*(5), 645–657.
32. **Thomas, D. D., et al.** (2008). The chemical biology of nitric oxide: implications in cellular signaling. *Free Radical Biology and Medicine*, *45*(1), 18–31.
33. Olatunji N. Salako[1], Idayat Shalewa Salako, Modupe Adebanji Akingbade et al. SodaSulphanecobalamin as a Broad-Spectrum Medical Countermeasure Agent for Chemical and Biological Threats: Synthesis, Safety, and Comparative Analysis, 07 October 2025, PREPRINT (Version 1) available at Research Square [https://doi.org/10.21203/rs.3.rs-7779935/v1]

Supplementary Files

This is a list of supplementary files associated with this preprint. Click to download.

- Supplementaryinformation.docx